AMERICAN SOCIETY FOR MICROBIOLOGY | Applied and Environmental Microbiology

Bacteriology | Full-Length Text

Glutamicibacter sp. ZY1 antagonizes pathogenic *Vibrio parahaemolyticus* via iron competition

Zhili Shi,[1,2] Ya Li,[1,2] Weibo Shi,[1,2] Zhixin Mu,[1,2] Qingxi Han,[1,2] Weiwei Zhang[1,2]

AUTHOR AFFILIATIONS See affiliation list on p. 16.

ABSTRACT Probiotics are prior agents for treating bacterial infection with advantages of inhibiting pathogenic bacteria and improving immune responses of hosts, thus increasing the survival rate of cultured animals. In this study, one *Vibrio parahaemolyticus* YDE17 pathogenic to shrimp and its antagonist *Glutamicibacter* sp. ZY1 were screened, and ZY1 showed stable inhibitory effects on diverse *Vibrio* spp., especially *V. parahaemolyticus*. ZY1 secreted inhibitory substances into supernatant, and the activity of inhibitory substances did not change after being treated under different temperatures, proteinase K, and pH (6-10), which indicated that the inhibitory substances might be small molecules, which led us to trace the siderophore production. The siderophore production of YDE17 co-incubated with the cell-free supernatant of ZY1 was greater than that of YDE17 alone, which indicated that the cell-free supernatant of ZY1 created iron-limiting conditions for YDE17. This finding was confirmed by iron supplementation assays, in which the inhibitory activity of the cell-free supernatant of ZY1 on YDE17 as well as the siderophore production of YDE17 decreased in the presence of $FeCl_3$. The effect of iron on inhibition was further confirmed by *in vivo* infection. The relative percent survival of ZY1 to shrimp challenged by YDE17 was 83.3%, but the survival rates of shrimp challenged with YDE17/ZY1/$FeCl_3$ were similar to that of YDE17, both of which were significantly lower than the 70% survival rate of shrimps simultaneously challenged by ZY1/YDE17. Our study offers a new probiotic resource to control vibriosis, which works through iron competition with the opportunistic pathogens of *Vibrio* spp.

IMPORTANCE Bacteria belonging to *Vibrio* spp., especially *Vibrio parahaemolyticus*, are important opportunistic pathogens infecting a wide range of hosts including fish, shrimp, shellfish, and crab. Antibiotics are effective but show the disadvantages of antibiotic generation, microecology destruction, and biological toxicology; thus, new treatments of *Vibrio* infection are urgently recommended. In our present study, *Glutamicibacter* sp. ZY1, belonging to the phylum Actinomycetes, was selected and showed high inhibitory activity to inhibit *V. parahaemolyticus* pathogenic to shrimp. *Glutamicibacter* sp. ZY1 antagonized *V. parahaemolyticus* YDE17 through producing siderophore to compete for iron, based on the results of both *in vitro* and in *vivo* experiments under different iron levels. This study offers a new strategy to control *Vibrio* infection in aquaculture.

KEYWORDS *Glutamicibacter* sp., *Vibrio parahaemolyticus*, iron competition, antagonism

China is a major producer of Pacific white shrimp (*Litopenaeus vannamei*) (1), but shrimp *L. vannamei* is highly susceptible to *Vibrio* spp. infections, and mass mortality occurs during its culture (2). The pathogenic strains that could infect shrimp *L. vannamei* include *Vibrio harveyi* (3), *Vibrio anguillarum* (4), *Vibrio alginolyticus* (5), *Vibrio parahaemolyticus* (6), and *Vibrio vulnificus* (7). To prevent or cure the infection of *Vibrio* spp., antibiotics have been frequently used; however, the excess and frequent use of

Editor Jennifer F. Biddle, University of Delaware, Lewes, Delaware, USA

Address correspondence to Weiwei Zhang, zhangweiwei1@nbu.edu.cn.

The authors declare that they have no known competing financial interests or personal relationships that could have appeared to influence the work reported in this paper.

See the funding table on p. 16.

Received 2 January 2025
Accepted 19 February 2025
Published 24 April 2025

antibiotics has caused several hazards, including the spread of drug-resistant genes, the generation of drug-resistant bacteria, and the destruction of microbial ecosystems (8, 9). Residual antibiotics can further affect the safety of animals and humans, as well as the stability of aquatic ecosystems (9). Recent reports indicate that the use of antibiotics in aquaculture should be replaced, emphasizing the urgency for strategies with necessary improvements to ensure aquaculture and human health (10).

Probiotic is an effective tool to treat the infection caused by *Vibrio* spp. (11). The selection of probiotics that antagonize *Vibrio* spp. and the identification of the inhibitory substances of probiotics against pathogens are vital for the application of probiotics (12). Currently, probiotics that antagonize *Vibrio* spp. are *Bacillus* (13), *Pseudomonas* (14), *Lactobacillus* (15), and *Streptococcus* (16), etc. Probiotics can achieve antagonistic effects by producing active inhibitory substances; striving for nutrients, chemicals, or energy; reducing virulence through the quorum-sensing system; and improving the digestion of macro-and/or micronutrients and the immunoregulatory capacity of the host (17, 18). The active inhibitory substances include bacteriocin, siderophores, lysozyme, proteolytic enzymes, and catalases, etc. (19). Particularly, iron is a key element for the growth and survival of almost all bacteria (20). Depriving iron from pathogenic bacteria is a ubiquitous antagonistic strategy between bacteria (21). Under iron-limiting conditions, bacteria can survive by secreting siderophores, which are low-molecular-weight substances that can bind ferric iron ions and transfer iron ions into the intracellular space of bacterial cells (22). In aquaculture, probiotics that use siderophores to compete for iron with pathogens include *Streptomyces* (23), the yeast *Aureobasidium pullulans* HN 6.2 (24), *Pseudomonas aeruginosa* PA1 (25), *Bacillus* sp. (26), and *Pseudomonas* sp. (27). *Streptomyces* are bacteria belonging to the phylum Actinomycetes and are promising biocontrol agents in aquaculture. *Streptomyces* can inhibit the opportunistic pathogen belonging to *Vibrio* spp., including *V. vulnificus*, *V. alginolyticus,* and *V. parahaemolyticus* (28). For example, the marine *Streptomyces* S073 could inhibit pathogenic *V. parahaemolyticus*, and this inhibition was attributed to the stronger iron chelating activity of S073 through the production of carboxylate siderophores, resulting in iron-limiting conditions for the pathogen (23).

In the present study, the bacterium ZY1, which exhibited inhibitory activity against a variety of *Vibrio* spp., was screened and identified. Subsequently, the inhibitory substances produced by ZY1 were traced and characterized. The preliminary mechanism on the antagonism of ZY1 on YDE17 was explored from the viewpoint of iron competition. Our results showed that the inhibitory effect of ZY1 on YDE17 was mainly due to its siderophore production to compete for iron, but YDE17 could compensate for limited iron to a certain degree by increasing siderophore production of itself. Finally, to determine whether ZY1 could protect shrimp from infection of *V. parahaemolyticus*, artificial infections using ZY1, YDE17, and simultaneous ZY1 and YDE17 under different iron levels were performed.

MATERIALS AND METHODS

Bacterial isolation

The water samples were collected from a diseased Pacific white shrimp farm in Jiangmen, Guangzhou. In the laboratory, 500 mL of the water samples was filtrated using a vacuum filter (JOANLAB, China). The bacteria on the membrane were resuspended in 5 mL sterilized seawater, and 50 µL of the cell suspension was spread on a 2216E agar plate. After incubation at 28°C for 24 h, several antagonistic circles were observed. The colonies of the inhibitory bacteria and bacteria surrounding the inhibitory circles were purified and identified. The bacterial status was identified according to the sequence of 16S ribosomal RNA (16S rRNA) gene, which was amplified by PCR using the universal primers of 27F (3′-GTGCTGCAGAGAGTTTGATCCTGGCTCAG-5′) and 1492R (3′-CACGGATC CTACGGGTACCTTGTTACGACTT-5′) (29). Briefly, cells of each bacterium were resuspended in ddH_2O and the suspensions were used as templates. PCR was performed in RCR

instrument (Bio-Gener, Hangzhou, China) with initial denaturation at 95°C for 2 min and 30 cycles of denaturation at 95°C for 30 s, annealing at 55°C for 30 s, extension at 72°C for 1 min, and a final extension step at 72°C for 10 min. The PCR products were sequenced by Youkang Biotechnology (Hangzhou, China), and the 16S rRNA sequences were aligned with known sequences in GenBank in NCBI using the BLAST. Phylogenetic analyses were implemented using the MEGA 11 software package, and phylogenetic trees were constructed using the neighbor-joining method (30).

Inhibitory spectrum of *Glutamicibacter* sp. ZY1

The antagonistic assay was performed using the disk diffusion method (31). The tested bacteria included strains belonging to *Splendidus* clade, *Vibrio mediterranei, Vibrio atlanticus, Coralliilyticus* clade, *Orientalis* clade, *Photobacterium* sp., *Nereis* clade, *Harveyi* clade, *Anguillarum* clade, *Aeromonas hydrophila*, *Pseudomonas aeruginosa*, *Escherichia coli*, *Enterobacter bugandensis*, *Morganella morganii*, *Cholerae* clade, *Pseudoalteromonas* sp., *Halomonas* sp., and *Klebsiella variicola*. All these strains were grown in 2216E medium, except that *P. aeruginosa* and *E. coli* were separately cultured in LB medium. All bacterial strains were preserved in our laboratory. All the strains were cultured to optical density at 600 nm (OD_{600}) of approximately 1.0 measured in a spectrophotometer (Allsheng, Hangzhou, China). Ten microliters of ZY1 was dropped on sterilized paper disks with a diameter of 0.6 cm and air dried. These filter paper disks were then put onto the bacterial lawn on the agar plates, and the plates were incubated at 28°C. After incubation overnight, the diameter of the inhibitory circle was measured. Each bacterium was independently cultured three times, and the antagonist assay was performed in triplicate for each tested bacterium.

Inhibitory activity of ZY1 on *V. parahaemolyticus* YDE17

To determine the optimal inhibitory ratio of ZY1 on YDE17 *in vitro*, the inhibitory activity of ZY1 on YDE17 was determined using the disk diffusion method with different bacterial cell ratios as described previously (31). Briefly, YDE17 and ZY1 were separately cultured in 2216E liquid medium until the OD_{600} reached approximately 1.0. YDE17 was 10-fold serially diluted with 2216E liquid medium, and the cell densities of suspensions ranged from 1×10^1 to 1×10^8 CFU/mL. One hundred microliters of each YDE17 dilution was spread onto the 2216E plate. ZY1 was also 10-fold serially diluted with 2216E liquid medium to make suspensions from 1×10^1 to 1×10^8 CFU/mL. Ten microliters of ZY1 was dropped on the sterilized filter paper disks and air dried. These filter paper disks were placed on 2216E agar plates with different cells of YDE17, and the plates were incubated at 28°C. After overnight incubation, the diameters of inhibitory circles were measured. Each bacterium was cultured three times to perform the inhibitory assay with three independent measurements.

Inhibition of YDE17 in seawater by ZY1

The inhibition of ZY1 on YDE17 in seawater was performed as described by Tang et al. (32). Briefly, ZY1 and YDE17 were separately cultured overnight until OD_{600} was 1.0. Four milliliters of ZY1 or YDE17 cultures was centrifuged at 12,000 rpm for 5 min, and the supernatant was filtered through a 0.22 µm pore size filter (Millipore, Darmstadt, Germany) to obtain two kinds of conditioned cell-free supernatant. Another 1.5-mL aliquot of the YDE17 culture was centrifuged at 12,000 rpm for 5 min, followed by resuspension of the cell pellet in 15 mL of sterilized seawater. The cell suspension of YDE17 was evenly divided into 24 aliquots, with 500 µL of each aliquot. The experimental groups were supplemented with 200 µL, 400 µL, 600 µL, and 800 µL of cell-free supernatant of ZY1, and the control groups were supplemented with 200 µL, 400 µL, 600 µL, and 800 µL of cell-free supernatant of YDE17, respectively. For each supplemented volume, three biological replicates were set. Finally, artificial sterilized seawater was added to make up to a total volume of 5 mL, and the 24 samples were incubated

statically at 28°C for 24 h. To count the cell number of YDE17 that remained in the seawater, the samples were 10-fold serially diluted using artificial sterilized seawater, and 10 µL of each dilution was dropped on 2216E agar plates. The plates were incubated at 28°C for 24 h, and the single colonies that appeared in one appropriate drop were counted.

Characterization of the inhibitory substance of ZY1

ZY1 and YDE17 were separately cultured overnight until OD_{600} reached 1.0. The culture of ZY1 was centrifuged at 12,000 rpm for 5 min, and the cell-free supernatant was obtained as described above. The cell-free supernatant of ZY1 was treated under different temperatures, proteinase K (Vazyme, Nanjing, China), and pHs, and the stability of the inhibitory substances under these conditions was then determined.

In order to determine the thermal stability of the inhibitory substances, cell-free supernatant of ZY1 was incubated at 40°C, 50°C, 60°C, 70°C, 80°C, 90°C, and 100°C for 1 h, respectively. The remaining inhibitory activity of cell-free supernatant of ZY1 was then determined at 28°C. To determine the effects of proteinase K on the inhibitory substances, cell-free supernatant of ZY1 was mixed with proteinase K at a ratio of 1:1 (vol/vol), incubated at 37°C for 1 h, then heated at 80°C for 10 min. The inhibitory activity of cell-free supernatant of ZY1 was then determined. To determine the pH stability of the inhibitory substances, the pHs of cell-free supernatant of ZY1 were subsequently adjusted to 4.0, 6.0, 8.0, 10.0, and 12.0 using 1 M HCl or 1 M NaOH and measured using a pH meter (Lei ci, Shanghai, China), respectively. After being incubated at different pHs for 1 h, the solution was adjusted back to the initial pH of 7.2 and was tested for the inhibitory activity. The bacterial lawn on the 2216E plate was prepared by mixing molten 2216E agar with 1% (vol/vol) culture of YDE17 at OD_{600} of 0.9 (33). For each experiment, independent replicates were performed for more than three times from the initial treatment under different conditions.

Inner membrane permeability

Based on the method described previously (34, 35), the β-galactosidase leaks outside of the cell and degrades the colorless *o*-nitrophenyl-β-D-galactopyranoside (ONPG, Solarbio, Beijing, China) to produce yellow *o*-nitrophenol and galactose when the inner membrane becomes permeable. Therefore, in this study, we evaluated the effect of the cell-free supernatant of ZY1 on the permeability of the inner membrane of YDE17 by the addition of ONPG. YDE17 and ZY1 were separately cultured overnight at 28°C to an OD_{600} of approximately 1.0, and the cultures were centrifuged at 10,000 rpm for 10 min. Cell-free supernatant of ZY1 was obtained as described above. The cell pellet of YDE17 was resuspended in the artificial sterilized seawater to make a cell suspension with OD_{600} of approximately 0.4. For the experimental group, 2 mL of cell-free supernatant of ZY1, 2 mL of YDE17 bacterial suspension, and 200 µL of ONPG solution (stock solution, 5 mg/mL) were mixed together. Two control groups were set, i.e., 2 mL artificial sterilized seawater instead of cell-free supernatant of ZY1 or YDE17 bacterial suspension. The reaction mixtures were shaken at 28°C and absorbance, at 420 nm was measured at a time interval of 1 h. Data were obtained from three independent replicates that were performed from the independent culture growth.

Measurement of siderophore level

The siderophore produced by bacteria was determined using the chrome azurol S (CAS) assay in both liquid medium and agar plate (36, 37). ZY1 was cultured in 2216E liquid medium at 28°C to different time intervals, and cell-free supernatant of ZY1 was obtained as described above. One milliliter of the cell-free supernatant from each culture, 1 mL of CAS bright blue dye, and 20 µL of shuttle solution were mixed. 2216E liquid medium, CAS dye, and shuttle solution were mixed and used as a control. The mixtures were incubated at room temperature for 5 min, followed by measurement of OD_{630} using

a spectrophotometer. Quantitative determination of siderophore levels was calculated using the following equation: siderophore% = [(Ar − As)/Ar] × 100, where Ar = absorbance of reference and As = absorbance of sample. For the qualitative determination, 100 µL of the cell-free supernatants of ZY1 at different OD_{600} values was dropped on the solid CAS agar plates (Hopebio, Qingdao, China), respectively. The appearance of the orange-yellow circle at the drop site was defined to be obvious production of siderophores, and the diameter of the orange-yellow circle was positively correlated with the level of the siderophores (23). More than three independent cultures were used for three independent measurements to determine the siderophore production.

To compare the siderophores produced by YDE17 with or without the cell-free supernatant of ZY1, the cell-free supernatant of ZY1 was collected at two cell densities: one was $OD_{600} \approx 0.7$ with no obvious siderophore production and the other was $OD_{600} \approx 0.9$ with obvious siderophore production observed on the CAS plate. Culture of YDE17 at OD_{600} of 1.0 was collected. Three samples, (i) 100 µL of the cell-free supernatant of ZY1 mixed with 100 µL of 2216E medium, (ii) 100 µL of YDE17 mixed with 100 µL of 2216E medium, and (iii) 100 µL of the cell-free supernatant of ZY1 mixed with 100 µL of YDE17 suspension, were simultaneously dropped on CAS agar plate. The plates were incubated at 28°C for 16 h, and the diameters of the orange-yellow circle were measured. Replicates were performed for more than three times from three independent cultures and measurements.

Determination of the type of siderophores produced by ZY1 and YDE17

Arnow's test (38), $FeCl_3$ experiment (39), and CAS test (40) were used to determine the types of siderophores produced by ZY1 and YDE17, respectively. YDE17 and ZY1 were separately cultured overnight at 28°C to an OD_{600} of approximately 1.0, and the cultures were centrifuged at 10,000 rpm for 10 min. Cell-free supernatants of ZY1 and YDE17 were obtained as described above. For Arnow's test, 1 mL supernatant/medium, 1 mL of 0.5 M HCl, 1 mL nitrate molybdate reagent (10 g $NaNO_2$ and 10 g Na_2MoO_4 dissolved in 100 mL ddH_2O), and 1 mL of 1 M NaOH were mixed. The mixture was incubated at room temperature for 5 min, and the color change of the solution was observed to indicate the catecholate siderophore. For the $FeCl_3$ experiment, 1 mL of the supernatant was subsequently supplemented with 1 or 5 mL of 2% $FeCl_3$ (Aladdin, Shanghai, China). If the solution immediately turns red when 1 mL of 2% $FeCl_3$ solution is added, it indicates that the supernatant contains the hydroxamate siderophore; if the supernatant only turns red or purple when 5 mL of 2% $FeCl_3$ solution is added, it indicates that the supernatant contains the catecholate siderophore. For the CAS test, 200 µL cell culture of ZY1 and YDE17 was separately dropped on a CAS plate. If the color changes to purple, the bacterium contains the catecholate siderophore; if the color changes to orange, the bacterium contains α-hydroxycarboxylates, i.e., vibrioferrin for *V. parahaemolyticus* (41); if the color changes to yellowish, the bacterium secretes carboxylate siderophore.

Effect of iron on inhibitory activity

To evaluate the effect of iron on inhibitory activity of cell-free supernatant of ZY1 on YDE17, cell-free supernatant of ZY1 with an OD_{600} of 0.9 was obtained as above. Cell-free supernatant of ZY1 was mixed with $FeCl_3$ at various concentrations, i.e., 200 µM, 400 µM, 600 µM and 800 µM, at a ratio of 1:1 (vol/vol) as described by Yang et al. (23). YDE17 was cultured overnight until OD_{600} was about 1.0, the YDE17 lawn was prepared, and the inhibitory assay was performed as described previously (33); then, the diameter of the inhibitory circle was measured. Independent cultures of ZY1 and YDE17 were grown for three times and were used for the triplicate inhibitory experiments.

Effect of iron on siderophore production

To determine whether iron level could affect the siderophore production, the change in color of YDE17 on a CAS agar plate was observed. Seven group samples were dropped

on the CAS plates: (i) 100 µL of the cell-free supernatant of ZY1 mixed with 100 µL of 2216E medium, (ii) 100 µL of YDE17 mixed with 100 µL of 2216E medium, (iii) 100 µL of the cell-free supernatant of ZY1 mixed with 100 µL of YDE17, (iv–vii) 100 µL of YDE17 supplemented with 100 µL of the cell-free supernatant of ZY1 and $FeCl_3$ at levels of 200 µM, 400 µM, 600 µM, and 800 µM, respectively. The seven samples were simultaneously dropped on CAS plates, and the diameter of the orange-yellow circle was measured. Independent cultures of ZY1 and YDE17 were separately grown for three times and were used for the triplicate experiments.

Artificial infections

Healthy Pacific white shrimp *L. vannamei* (mean length, 1 ± 0.03 cm) were purchased from the Mei Tai shrimp farm in Zhuhai, Guangzhou. They were cultured at 27°C for 7 days with air inflation, then the shrimps were challenged by different bacterial combinations using immersion infection mode. The shrimps were fed with basic feed four times a day. To calculate the mean lethal doses (LD_{50}) of YDE17, 1,350 shrimps were divided into 27 groups with 50 shrimps in each groupShrimps were infected with YDE17 at concentrations of 5×10^4 CFU/mL, 1.25×10^5 CFU/mL, 2.5×10^5 CFU/mL, 5×10^5 CFU/mL, 1.25×10^6 CFU/mL, 6.25×10^6 CFU/mL, 3.125×10^7 CFU/mL, and 1.5×10^8 CFU/mL, while the control group was supplemented with the same volume of sterilized 2216E medium. For each bacterial concentration, three groups of shrimps were parallelly infected. The health status of shrimps was observed every 8 h for 5 days, and the number of dead shrimps was recorded. The LD_{50} of YDE17 were calculated using the Karber method (42). There were a few deaths of shrimps challenged by 1×10^5 CFU/mL ZY1 in the preliminary experiment; thus, ZY1 at this concentration was used in the protective test. To demonstrate whether ZY1 exerts a protective effect, 600 shrimps were randomly divided into 12 groups with 50 shrimps in each group. The groups were separately challenged with YDE17 (1×10^6 CFU/mL), ZY1 (1×10^5 CFU/mL), ZY1 (1×10^5 CFU/mL)/YDE17 (1×10^6 CFU/mL), and a control group without bacterial inoculation. For each immersion infection, three replicates were performed. The clinical symptoms of individuals were observed, and the number of dead shrimps in each group was recorded. To further determine the effect of $FeCl_3$ on the inhibitory effect of ZY1 *in vivo,* 800 µM $FeCl_3$ and 40 µM 2,2-bipyridyl (DP, iron chelator, Macklin, Shanghai, China) were also used in the subsequent infection experiment. Seven hundred fifty shrimps were randomly divided into 15 groups with 50 shrimps in each group. The groups were YDE17 (1×10^6 CFU/mL)/ZY1 (1×10^5 CFU/mL)/$FeCl_3$, YDE17 (1×10^6 CFU/mL)/DP, $FeCl_3$, DP and a control group without any treatment. Three replicates were performed for each group. Individuals were observed for clinical signs, and the number of dead shrimps in each group was recorded. The following formula was used to calculate survival rate (%) and relative percent survival (RPS, %) (43) :

$$\text{survival rate}\,(\%) = 100 \times \frac{\text{Survival number of each treatment after challenge}}{\text{Total number before challenge}};$$

$$\text{RPS}\,(\%) = 100 \times \left(1 - \frac{\text{Mortality rate of the co} - \text{infected group}}{\text{Mortality rate of YDE17 group}}\right).$$

Statistical analysis

All data were obtained in triplicate with similar results. Statistical analyses were carried out using GraphPad Prism (GraphPad Software). The two-tailed unpaired Student's *t*-test was used to analyze all data, except for the determination of survival rate. Data were presented as mean ± standard deviation (SD). In all cases, differences were defined as *, $P < 0.05$; **, $P < 0.01$; ***, $P < 0.001$, and ****, $P < 0.0001$.

RESULTS

Screening, isolation, and characterization of antagonistic bacteria

In the water samples collected from the shrimp farm, 21 species of culturable strains were isolated and identified (Table S1). Among them, the inhibitory effect of ZY1 on YDE17 was demonstrated with the largest inhibition zone (Fig. 1A). Furthermore, the cell-free supernatant of ZY1 had the same antagonistic effect as the intact cells (Fig. 1B). The 16S rRNA gene sequence of YDE17 and subsequent phylogenetic analysis indicated that YDE17 was *V. parahaemolyticus*, with homology to the *V. parahaemolyticus* strain ATCC 17802 (Fig. 1C). The 16S rRNA gene sequence of ZY1 and subsequent phylogenetic analysis indicated that ZY1 belonged to the *Glutamicibacter soli*, which is homologous to the *G. soli* strain SYB2 (Fig. 1D).

Inhibitory spectrum of *Glutamicibacter* sp. ZY1

To determine the inhibitory spectrum of ZY1, 28 different species of bacteria were used to perform the inhibitory assay on 2216E or LB agar plates. ZY1 antagonized many kinds of bacteria, including the *Splendidus* clade, *Coralliilyticus* clade, *Orientalis* clade, *Photobacterium* sp., *Harveyi* clade, *Anguillarum* clade, and *Pseudoalteromonas* sp., but could not antagonize the *Nereis* clade, *Cholerae* clade, *V. atlanticus*, *A. hydrophila*, *P. aeruginosa*, *E. coli*, *E. bugandensis*, *M. morganii*, *Halomonas* sp., and *K. variicola* strains (Table 1; Fig. S1).

Inhibitory effect of ZY1 on the growth of YDE17 in different matrices

The inhibitory effect of ZY1 on the growth of YDE17 was in a dose-dependent manner. When more ZY1 co-incubated with less YDE17, it showed the larger inhibitory circle. In detail, the cells of YDE17 below 1×10^4 CFU could not be grown to lawns, while even if there were as few as 1×10^3 CFU bacterial cells of ZY1, it exhibited inhibitory activity on

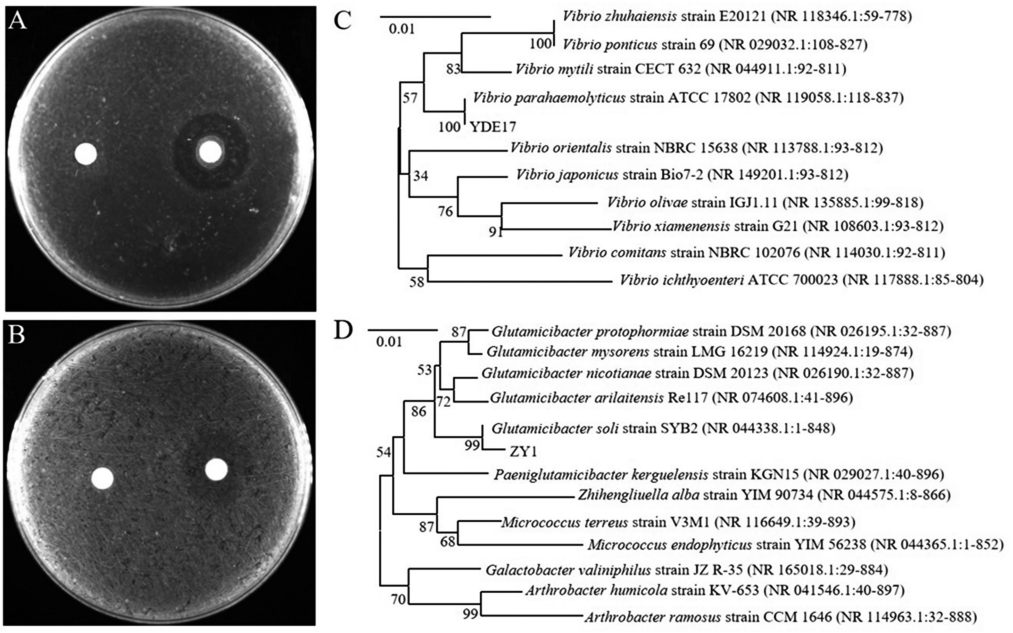

FIG 1 Bacterial isolation and identification. (A) Strain ZY1 antagonized YDE17. Fifty microliters of YDE17 was spread on 2216E plate, with the filter disk dipped with 2216E (left) and filter disk dipped with ZY1 cultured in 2216E medium (right), and the plate was incubated at 28°C for 24 h. (B) Cell-free supernatant of ZY1 antagonized YDE17. Fifty microliters of YDE17 was spread on 2216E plate, with the filter disk dipped with 2216E (left) and filter disk dipped with cell-free supernatant of ZY1 cultured in 2216E medium (right), and the plate was incubated at 28°C for 24 h. (C) Phylogenetic tree of YDE17 constructed using 16S rRNA. (D) Phylogenetic tree of ZY1 constructed using 16S rRNA.

TABLE 1 Strains used to determine the inhibitory spectrum of ZY1[a]

Strain name	Clade	Genus/species name (with high similarity)	Size of the antagonistic zone/cm (mean ± SD)
AJ01	Splendidus	*Vibrio splendidus*	2.2 ± 0.1
S1		*V. mediterranei*	1.3 ± 0.3
S2	Splendidus	*V. crassostreae*; *V. coralliirubri*; *V. gigantis*	2.87 ± 0.07
S7		*V. atlanticus*; *V. cyclitrophicus*; *V. tasmaniensis*	0.6
S8	Splendidus	*V. crassostreae*; *V. pomeroyi*; *V. cyclitrophicus*	2.03 ± 0.03
Y10n	Splendidus	*V. pelagius*; *V. fortis*; *V. xiamenensis*	2.73 ± 0.12
SPS2	Coralliilyticus	*V. coralliilyticus*	2.33 ± 0.03
SPS11	Orientalis	*V. brasiliensis*	2.40 ± 0.10
PTS6		*Photobacterium ganghwense*	1.97 ± 0.04
Y1n	Nereis	*V. nereis*; *V. hepatarius*; *V. coralliilyticus*	0.6
Y3n	Nereis	*V. nereis*	0.6
G2	Harveyi	*V. alginolyticus*; *V. owensii*; *V. hyugaensis*	2.4 ± 0.1
H1	Harveyi	*V. alginolyticus*	1.4 ± 0
Y9n-1	Harveyi	*V. natriegens*; *V. alginolyticus*	1.33 ± 0.07
G3n	Harveyi	*V. rotiferianus*	2.43 ± 0.04
Sps1	Harveyi	*V. parahaemolyticus*	1.37 ± 0.12
W3	Harveyi	*V. jasicida*; *V. owensii*; *V. rotiferianus*	2.00 ± 0.01
Va01	Anguillarum	*V. anguillarum*	2.93 ± 0.04
YD17		*Aeromonas hydrophila*	0.6
PA		*Pseudomonas aeruginosa*	0.6
DH5α		*Escherichia coli*	0.6
YD6		*Enterobacter bugandensis*	0.6
YD9		*Morganella morganii*	0.6
YDE13	Cholerae	*V. cholerae*	0.6
H2		*Pseudoalteromonas* sp.	2.06 ± 0.04
NTS6		*Halomonas* sp.	0.6
YH4		*Klebsiella variicola*	0.6

[a]The size of the inhibitory circle included the diameter of the filter disk (0.6 cm).

the thinnest YDE17 lawn grown from the 1×10^4 CFU. The inhibitory effect of ZY1 could steadily be detected when the cell numbers were more than 1×10^5 CFU, regardless of the level of YDE17 on the agar plates. The largest inhibitory circle appeared when the cell number of ZY1 was 1×10^8 CFU and the cell number of YDE17 was 1×10^4 CFU (Table 2; Fig. S2). Furthermore, to test whether this inhibition could occur in the real seawater sample, the cell-free supernatant of ZY1 was applied to YDE17 suspension in artificial seawater. As the volume of the cell-free supernatant of ZY1 increased, the number of YDE17 cells gradually decreased, indicating that the cell-free supernatant of ZY1 could inhibit YDE17 cells. When the volume of the cell-free supernatant of ZY1 reached 800 µL, the cell number of YDE17 was only 8×10^5 CFU, but the cell number of YDE17 in the control group was approximately 2.8×10^6 CFU (Fig. 2), which indicated that the growth of *V. parahaemolyticus* YDE17 could be inhibited by approximately 72% in the presence of the cell-free supernatant of ZY1.

Characterization of the inhibitory effect of ZY1

Since the cell-free supernatant of the ZY1 culture had an inhibitory effect, it was used to characterize the inhibitory activity under different treatments. After treatment under different temperatures, the inhibitory activity of the cell-free supernatant of ZY1 did not change (Fig. 3A and B). To determine the effect of proteinase K, the inhibitory activity of the cell-free supernatant of ZY1 with and without proteinase K treatment was compared. The results showed that the inhibitory activity of the cell-free supernatant of ZY1 hardly

TABLE 2 Diameters of the inhibitory circle of ZY1 on the YDE17 lawn at different cell ratios[c]

	Diameter at YDE17[a] ratio of:							
ZY1[b] ratio	10^1	10^2	10^3	10^4	10^5	10^6	10^7	10^8
10^1	0.6	0.6	0.6	0.6	0.6	0.6	0.6	0.6
10^2	0.6	0.6	0.6	0.6	0.6	0.6	0.6	0.6
10^3	0.6	0.6	0.6	1 ± 0.01	0.6	0.6	0.6	0.6
10^4	0.6	0.6	0.6	1.1 ± 0.01	0.6	0.6	0.6	0.6
10^5	0.6	0.6	0.6	2 ± 0.02	2 ± 0.01	0.9 ± 0.01	1 ± 0.02	0.9 ± 0.01
10^6	0.6	0.6	0.6	2.3 ± 0.02	2 ± 0.01	1.4 ± 0.01	1.4 ± 0.01	1.4 ± 0.01
10^7	0.6	0.6	0.6	3.1 ± 0.01	2.5 ± 0.03	1.9 ± 0.02	1.8 ± 0.02	1.7 ± 0.02
10^8	0.6	0.6	0.6	3.6 ± 0.01	2.7 ± 0.02	2.2 ± 0.01	1.9 ± 0.02	1.9 ± 0.03

[a]The cell density of YDE17 suspension (indicated in the first row) and 100 µL of each dilution were spread on each plate.
[b]The cell density of ZY1 suspension (indicated in the first column) and 10 µL of each dilution were dropped onto the filter disk.
[c]The diameters of the inhibitory circle included the diameter of the filter disk, which is 0.6 cm.

changed after treatment with proteinase K (Fig. 3C). After treatment under different pHs ranging from 6 to 10, the inhibitory activity remained, but extremely acidic and alkaline conditions decreased the inhibitory activity of the cell-free supernatant of ZY1 (Fig. 3D and E).

β-galactosidase result showed that the absorbance of YDE17 co-incubated with the cell-free supernatant of ZY1 increased, but the absorbance of the control group barely changed (Fig. 3F). The samples were colorless before the reaction, but after incubation for 3 h, the color of the reaction mixture with YDE17 and the cell-free supernatant of ZY1 changed to yellow; however, the two control groups remained colorless (Fig. 3G and H). These results indicated that the cell-free supernatant of ZY1 could damage the inner membrane of YDE17 cells.

In summary, the inhibitory activity of the cell-free supernatant of ZY1 exhibited the following characteristics: thermal stability, proteinase K stability, and pH stability within the range of 6–10. These characteristics led us to speculate that the inhibitory substances in the cell-free supernatant of ZY1 were small and nonprotein molecules. Since iron competition is the strategy usually occupied by probiotics, we further wonder whether the siderophores produced by ZY1 were the functional inhibitory substances on YDE17.

ZY1 inhibited YDE17 through siderophore production to compete for iron

The siderophore level in the supernatant of ZY1 was cell density dependent, with a trend of first increasing and then decreasing. When ZY1 was cultured to an OD_{600}≈0.9, the siderophore level reached a maximum level, then, the level of siderophore decreased. When the OD_{600} of ZY1 was less than 0.7, the level of siderophores was lower (Fig. 4A). CAS assays showed that the color on the CAS plate did not change when the cell-free supernatant of ZY1 at OD_{600} ≈0.4 was dropped (Fig. 4Bi); however, the color on the CAS plate changed to orange-yellow when the cell-free supernatant of ZY1 at OD_{600} ≈0.9 was dropped (Fig. 4Bii). Taken all the results together, it can be deduced that the inhibition of ZY1 on YDE17 might be attributed to the siderophores produced by ZY1, which created an iron-limiting condition for YDE17. To verify this postulation, the siderophore production of YDE17 in the presence of the cell-free supernatant of ZY1 was determined. The results showed that when the cell-free supernatant of ZY1 at an OD_{600} ≈ 0.7 with no color change was supplemented, the orange-yellow circle of YDE17 was larger than that without the cell-free supernatant. The similar phenomenon was also observed when the cell-free supernatant of ZY1 at an OD_{600} ≈ 0.9 was collected and applied (Fig. 4C). Therefore, the presence of the cell-free supernatant of ZY1 likely induced the siderophore secretion of YDE17, which could also support the incomplete inhibition of YDE17 growth by ZY1 vice versa.

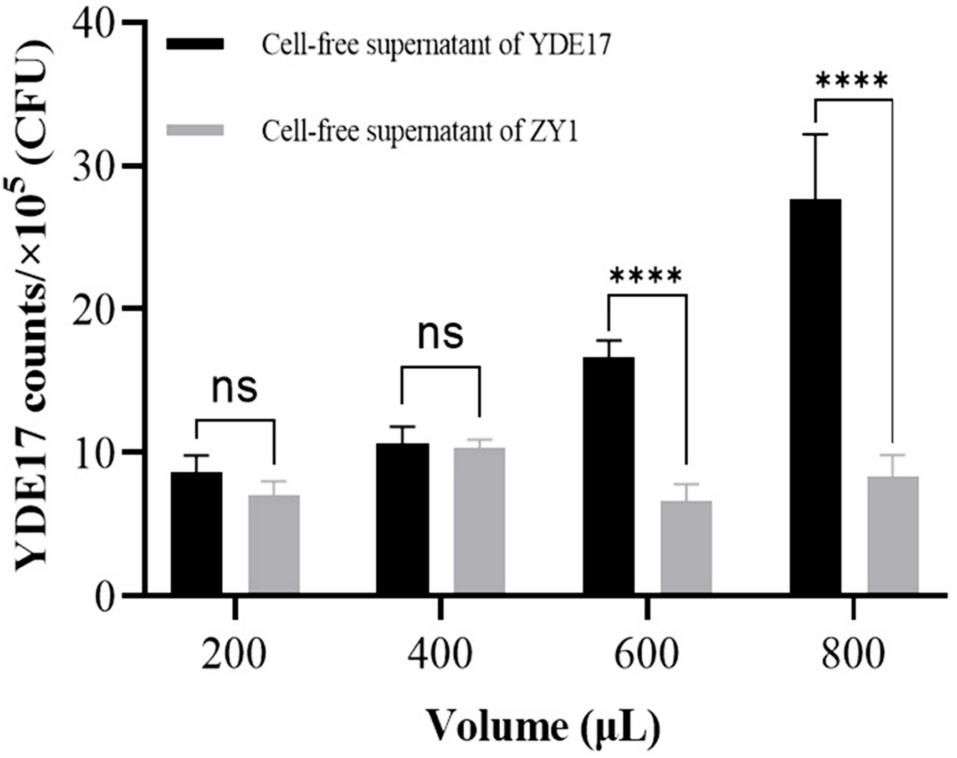

FIG 2 Inhibition of YDE17 by the cell-free supernatant of ZY1 in artificial seawater. Different volumes of the cell-free supernatant of ZY1 were supplemented into the YDE17 suspension in seawater, and the cell-free supernatant of YDE17 itself was also supplemented as a control. For each addition volume, three biological replicates were performed. The 24 samples were incubated at 28°C for 24 h, and the cells of remaining YDE17 in the artificial seawater were numbered using the dropped plate method. Data are mean values ± SD. ****, $P < 0.0001$.

To further confirm that the inhibitory effect of ZY1 was exerted by iron competition, the inhibitory assay was performed with $FeCl_3$ supplementation. $FeCl_3$ concentrations of 200 µM, 400 µM, 600 µM, and 800 µM were tested, and none of which affected the growth of YDE17 (Fig. S3A). As the levels of $FeCl_3$ in the cell-free supernatant of ZY1 increased, the inhibitory circle decreased. When the $FeCl_3$ concentration increased to 800 µM, the inhibitory circle completely disappeared (Fig. 4D; Fig. S3B through F). Thus, the inhibitory effect of ZY1 on the growth of YDE17 was mainly attributed to iron competition.

ZY1 produced hydroxamate and α-hydroxycarboxylate siderophores, while YDE17 produced vibrioferrin

Because the siderophores played important roles in the competition between the two bacteria, the types of siderophores produced by both strains were further determined. In the Anow's test, the color of the solution did not change to red after the addition of cell-free supernatant ZY1 or cell-free supernatant YDE17, indicating that the siderophore produced by both strains was not the catecholate type (Fig. 5A). In the $FeCl_3$ test, the color of the solution changed to red when 1 mL of $FeCl_3$ was added to cell-free supernatant of ZY1 (Fig. 5Bii), indicating that ZY1 produced the hydroxamate siderophore, but there was no change in the color whether 1 mL or 5 mL $FeCl_3$ was added into the supernatant of YDE17 (Fig. 5Biii), indicating that YDE17 did not produce the hydroxamate siderophore or the catecholate siderophore. In the CAS experiment, the color of the CAS plate changed from blue to orange, indicating that the ZY1 secreted the α-hydroxycarboxylate siderophore and YDE17 secreted vibrioferrin (Fig. 5C and D).

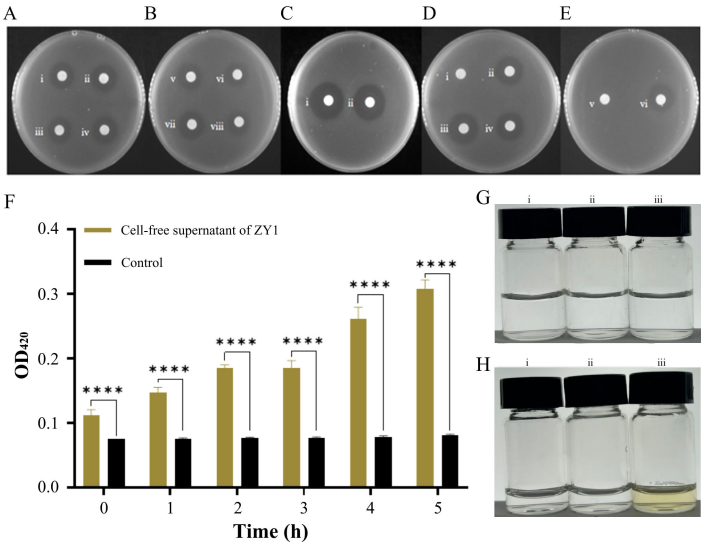

FIG 3 Characterization of the inhibitory activity of the cell-free supernatant of ZY1. (A and B) The inhibitory activity of the cell-free supernatant of ZY1 treated at different temperatures. The numbers "i, ii, iii, iv, v, vi, and vii" represented the cell-free supernatant of ZY1 treated under 40°C, 50°C, 60°C, 70°C, 80°C, 90°C, and 100°C, respectively, the number "viii" represented the cell-free supernatant of ZY1 without treatment. (C) The inhibitory activity of the cell-free supernatant of ZY1 treated with proteinase K. The number "i" represented the cell-free supernatant of ZY1 without treatment, "ii" represented the cell-free supernatant of ZY1 treated with proteinase K. (D and E) The inhibitory activity of the cell-free supernatant of ZY1 treated under different pHs. The numbers "i, ii, iii, iv, and v" represented pH = 4, 6, 8, 10, and 12, respectively. The number "vi" represented the cell-free supernatant of ZY1 without treatment. (F) Inner membrane permeability of YDE17 treated with the cell-free supernatant of ZY1; control: 2 mL of artificial seawater mixed with 2 mL of YDE17 and 200 µL of ONPG; cell-free supernatant of ZY1: 2 mL of the cell-free supernatant of ZY1, 2 mL of YDE17, and 200 µL of ONPG. (G) Color of the samples before reaction. (H) Color of the samples after the reaction for 3 h. (i) 2 mL of cell-free supernatant of ZY1 mixed with 2 mL of seawater and 200 µL of ONPG; (ii) 2 mL of YDE17 mixed with 2 mL of artificial seawater and 200 µL of ONPG; (iii) 2 mL of cell-free supernatant of ZY1, 2 mL of YDE17 and 200 µL of ONPG. All the measurements were performed in triplicate from three independent cultures. Data are mean values ± SD. ****, $P < 0.0001$.

The siderophore production of both strains in the presence of iron was further determined. $FeCl_3$ at concentrations of 200 µM, 400 µM, 600 µM, and 800 µM was used. Then, cell-free supernatant of ZY1 with or without $FeCl_3$ was applied to YDE17, and the siderophore production was detected. The results showed that as the $FeCl_3$ concentration in the cell-free supernatant of ZY1 increased, the orange-yellow circle of YDE17 decreased, and the orange-yellow circle nearly disappeared when the concentration of $FeCl_3$ was 800 µM (Fig. 6).

ZY1 protected shrimp from YDE17 infection

When challenged by different concentrations of YDE17, the survival rate of shrimp *L. vannamei* decreased as concentrations of YDE17 increased (Table 3). The infected shrimp showed signs of jejunum followed by whitening of the entire shrimp body and death. On the basis of these results, the LD_{50} of YDE17 was calculated as 1×10^6 CFU/mL in the artificial immerse infection mode. In the group infected with ZY1 alone, the average survival rate of the shrimp was 86%, which indicated that ZY1 was relatively safe for shrimp. In the ZY1/YDE17 group, the shrimp started to die on the 3rd day, and the survival rate reached 90% on the 5th day. In the group infected with YDE17 alone, the survival rate of the shrimp was 40% (Fig. 7A). On the basis of these data, the RPS of ZY1 was calculated as 83.3%. Thus, ZY1 could protect shrimp from YDE17 infection.

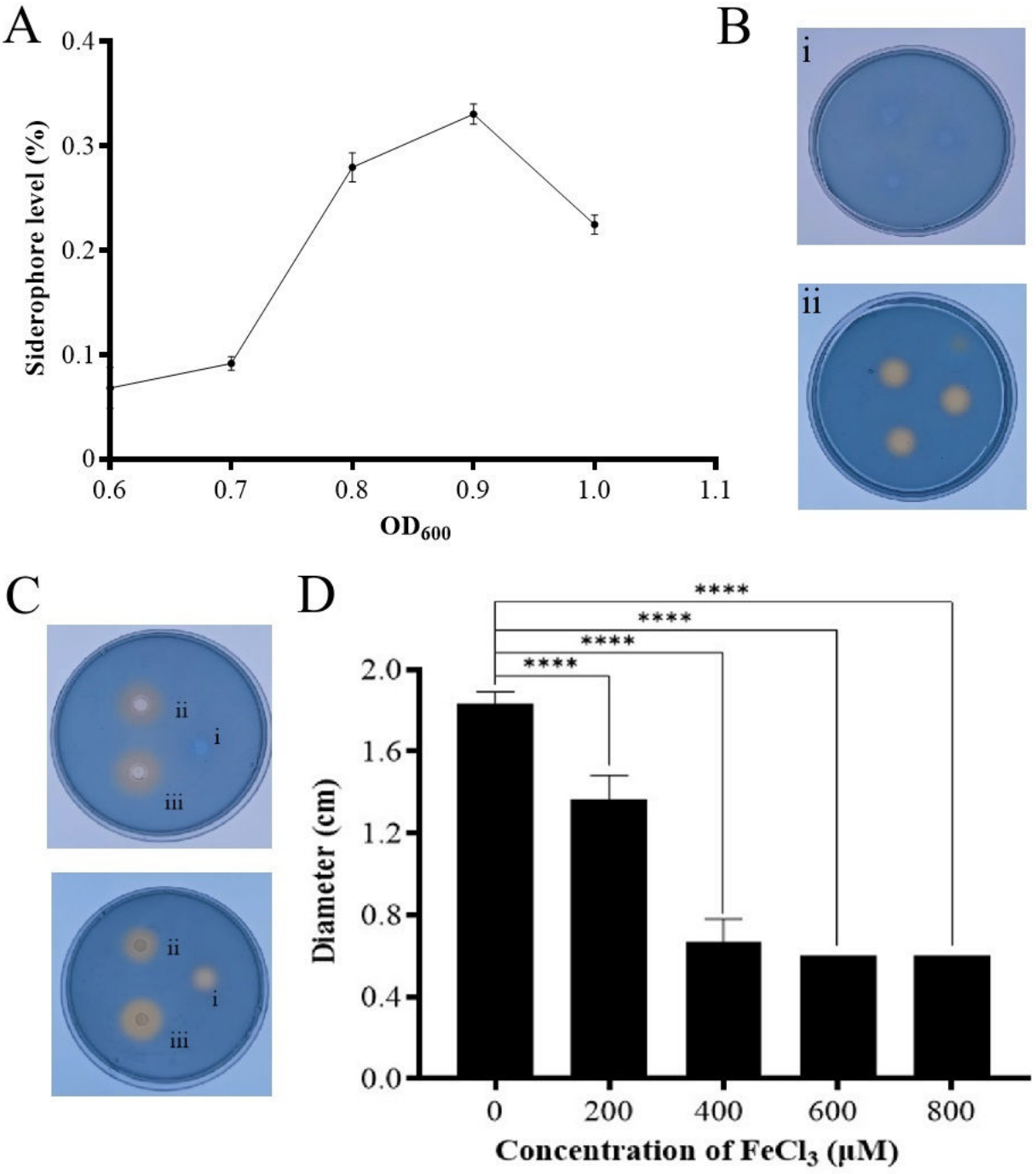

FIG 4 Siderophore productions of ZY1 and YED17 under different conditions. (A) Siderophore levels of ZY1 at different OD_{600} values. (B) The cell-free supernatant of ZY1 at different OD_{600} dropped on CAS plates: (i) the three replicates of cell-free supernatant of ZY1 at an OD_{600} of 0.4 dropped on a CAS plate; (ii) the three replicates of cell-free supernatant of ZY1 at an OD_{600} of 0.9 dropped on a CAS plate. (C) The effect of cell-free supernatant of ZY1 on the siderophore production of YDE17. The cell-free supernatant was obtained from ZY1 at an OD_{600} of 0.7 (upper): (i) the cell-free supernatant of ZY1, (ii) YDE17 suspension, and (iii) the cell suspension of YDE17 mixed with the cell-free supernatant of ZY1 dropped on a CAS plate. (C) The cell-free supernatant was obtained from ZY1 at an OD_{600} of 0.9 (lower): (i) the cell-free supernatant of ZY1, (ii) YDE17 suspension, and (iii) the cell suspension of YDE17 mixed with the cell-free supernatant of ZY1 dropped on a CAS plate. (D) Diameters of the inhibitory circle generated by cell-free supernatant of ZY1 with different concentrations of $FeCl_3$. The diameter of the inhibitory circle included the diameter of the filter paper sheet (0.6 cm). The data are the mean values of three replicates ± SD. ****, $P < 0.0001$.

To determine the effect of $FeCl_3$ on the inhibitory activity of ZY1 *in vivo*, the infection with different bacterial strains under different iron conditions was performed. $FeCl_3$

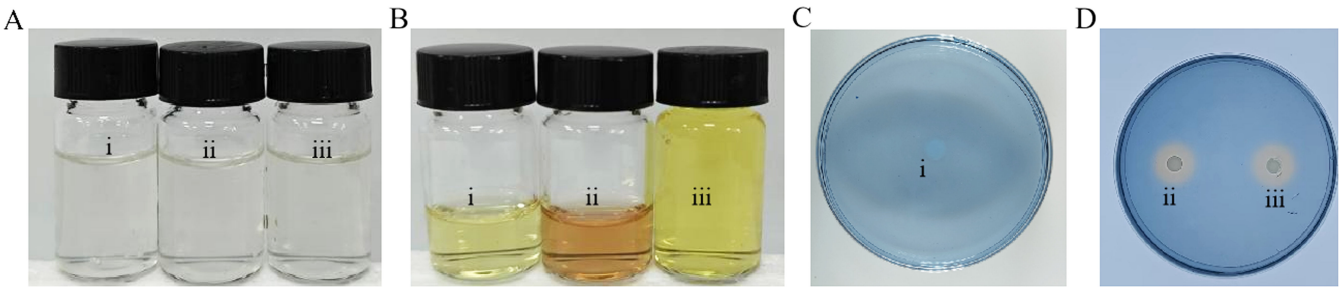

FIG 5 Determination of the siderophore production of ZY1 and YDE17. (A) Anow's test: (i) the control 2216E medium; (ii) cell-free supernatant of ZY1; (iii) cell-free supernatant of YDE17. (B) $FeCl_3$ test: (i) the control 2216E medium; (ii) cell-free supernatant of ZY1; (iii) cell-free supernatant of YDE17. (C and D) CAS test: (i) the control 2216E medium; (ii) cell culture of ZY1; (iii) cell culture of YDE17.

showed a minor effect on the survival rates, but the shrimps treated with DP at the level without affection of growth of YDE17 (data not shown) showed a survival rate of 38%, which indicated that iron is important for the survival of shrimps. The survival rate of shrimp challenged with YDE17/ZY1/$FeCl_3$ was 6%, which was significantly lower than 90% challenged with the co-infection of ZY1/YDE17 (Fig. 7B). This result indicated that the protective effect of ZY1 on YDE17 infection was regulated by iron level, and no protective effect was detected at higher iron levels in the *in vivo* immerse infection model.

DISCUSSION

Actinomycetes are considered producers of a broad spectrum of antagonistic compounds or extracellular enzymes, and they are considered ideal probiotic candidates in aquaculture (44–46). Previously, the potential actinobacterial genera were limited to *Streptomyces*, *Micromonospora*, and *Salinispora* (45). The genus *Glutamicibacter* is an actinobacteria belonging to the family Micrococcaceae (47), and it is known for their production of antibiotics and enzymes that play crucial roles in the treatment of chronic human diseases (48). Studies have shown that *Glutamicibacter uratoxydans* KIBGEIB41 produces chitinase that hydrolyzes the cell wall of the fungus, increasing the resistance of the organism to the fungus (49). The *Glutamicibacter bergerei* 04–279 strain inhibits fish pathogens such as *V. anguillarum* and *Photobacterium damselae* (50). However, only a few studies have explored the antagonistic effects of *Glutamicibacter* sp. and active

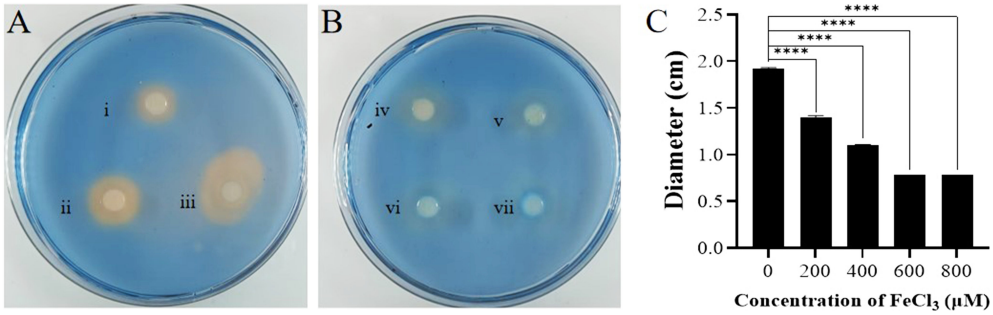

FIG 6 Effects of the cell-free supernatant of ZY1 on the siderophore production of YDE17 with different concentrations of $FeCl_3$. (A) The siderophore productions of (i) cell-free supernatant of ZY1; (ii) YDE17 cells; (iii) YDE17 cells with the cell-free supernatant of ZY1. (B) The siderophore productions of (iv) YDE17 cells with the cell-free supernatant of ZY1 and 200 µM of $FeCl_3$; (v) YDE17 cells with the cell-free supernatant of ZY1 and 400 µM of $FeCl_3$; (vi) YDE17 cells with the cell-free supernatant of ZY1 and 600 µM of $FeCl_3$; (vii) YDE17 cells with the cell-free supernatant of ZY1 and 800 µM of $FeCl_3$. (C) Diameter of the orange-yellow color of (iii–vii) in the above figures. The diameter of the orange-yellow color included the diameter of the filter disk, which was 0.6 cm. All the measurements were performed in triplicate from three independent cultures. The data are presented as the means ± SD. ****, $P < 0.0001$.

TABLE 3 Survival of shrimp *Litopenaeus vannamei* challenged by different levels of YDE17

Concentration of YDE17 (CFU/mL)	Survival rate (%)
5.00×10^4	100
1.25×10^5	74
2.50×10^5	72
5.00×10^5	62
1.25×10^6	0
6.25×10^6	0
3.13×10^7	0
1.50×10^8	0

substances produced by *Glutamicibacter* sp. (51). Our study is the first to identify a *Glutamicibacter* sp. with the capacity to inhibit a diverse of pathogenic *Vibrio* spp., including a *V. parahaemolyticus* isolate that was highly virulent to shrimp. ZY1 exhibited a broad spectrum of inhibitory effects on *Vibrio* spp., and it exhibited an average diameter of 2.15 cm. The inhibitory ability of ZY1 was positively correlated with cell number, which was similar to the cell density-dependent inhibitory effects of *Lactiplantibacillus plantarum* and *Pediococcus acidilactici* on *Vibrio* spp. (52).

The role of siderophores in improving antimicrobial properties has become a popular research topic in recent years (20). For example, *Streptomyces* can inhibit the growth of *Vibrio* sp. by producing siderophores (53). In bacteria belonging to *Glutamicibacter* sp., the antimicrobial substances kinetin-9-ribose and embinin, produced by *Glutamicibacter mysorens* (48), and unknown molecules, produced by *Glutamicibacter* sp. FBE-19 (54), have been reported, but there have been no reports on the inhibition of pathogens via iron competition using siderophore production. The thermal stability, pH, and proteinase K stability of the inhibitory substrates indicated that the inhibitory substances were small and nonprotein molecules, similar to previous findings in *Streptomyces* sp. S073 and *Bacillus subtilis* strain O-741 (23, 55). With the attenuated inhibitory effect in the presence of increased iron levels, we postulated that the inhibitory substances produced by ZY1 were siderophores, through which ZY1 inhibited YDE17 via iron competition. However,

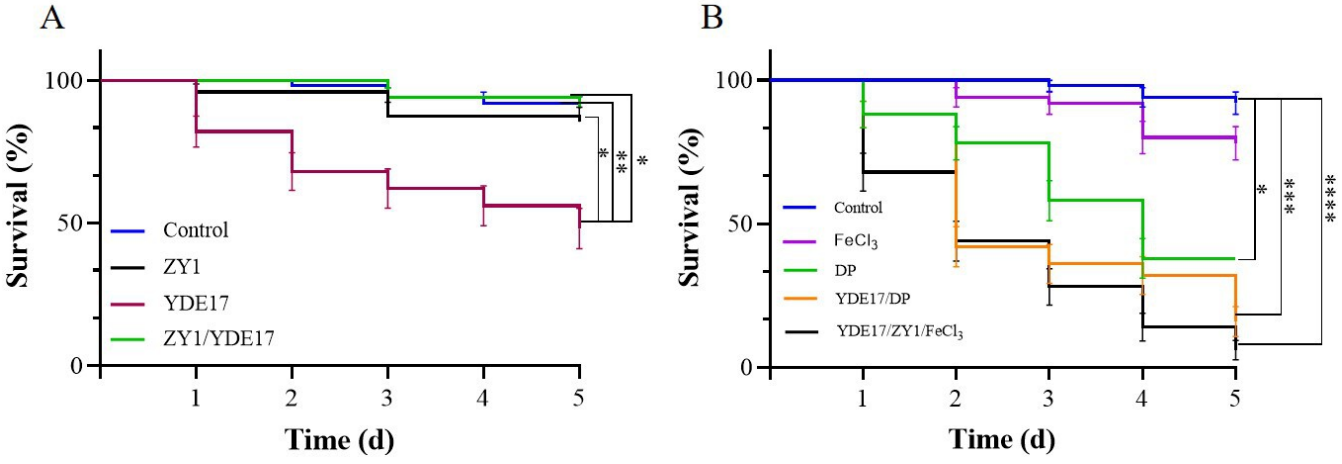

FIG 7 Survival rates of the different groups of shrimps. (A) The control group, the shrimp in seawater supplemented with 2216E medium; the YDE17 group, the shrimp challenged with 10^6 CFU/mL YDE17; the ZY1 group, the shrimp challenged with 10^5 CFU/mL ZY1; and the ZY1/YDE17 group, the shrimp simultaneously challenged with 10^6 CFU/mL YDE17 and 10^5 CFU/mL ZY1. All the groups were observed for 5 days, and the number of dead individuals was recorded. (B) The effect of iron on the infection of *V. parahaemolyticus in vivo*. The control group, the shrimp in water supplemented with 2216E medium; the $FeCl_3$ group, the shrimp challenged with 800 µM $FeCl_3$; the DP group, the shrimp challenged with 40 µM DP; the YDE17/DP group, the shrimp challenged with 10^6 CFU/mL YDE17 and 40 µM DP; the YDE17/ZY1/$FeCl_3$ group, the shrimp challenged with 10^6 CFU/mL YDE17, 10^5 CFU/mL ZY1, and 800 µM $FeCl_3$. Shrimps in all the groups were observed for 5 days, and the number of dead individuals was recorded. The data are presented as the means ± SD. *, $P < 0.05$; **, $P < 0.01$; ***, $P < 0.001$; ****, $P < 0.0001$.

unlike the complete inhibitory effects of *Streptomyces* (23), *Bacillus* sp. JK08 (56), and LAB (57) on *Vibrio* sp., the inhibitory effect of ZY1 was incomplete, which indicated that the inhibitory effect of ZY1 could induce a quick response of YDE17. The greater amount of siderophores produced by YDE17 in the presence of the cell-free supernatant of ZY1 further confirmed that YDE17 could produce more siderophores under the iron-limiting conditions created by the cell-free supernatant of ZY1, allowing the remaining bacterial cells to survive. This finding is consistent with the common knowledge that bacteria have the capacity to produce more siderophores under the iron-limiting condition created by iron chelator 2,2-bipyridyl (58). Depending on the chemical nature of the ligand that provides oxygen for Fe(III) coordination, siderophores can be classified into catecholates, hydroxamates, carboxylates, α-hydroxycarboxylates, or a mixture of types integrating the characteristics of at least two of them (59). The type of siderophore produced by ZY1 was the same as those produced by *Streptomyces* sp. S073 (23), which is α-hydroxycarboxylate. In addition, ZY1 produces another hydroxamate siderophore. YDE17 secretes only one kind of siderophore, vibrioferrin, according to the previous reports and our present study (41).

Vibrio spp., including *V. alginolyticus*, *V. anguillarum*, *V. harveyi,* and *V. parahaemolyticus*, are the main bacterial species that cause vibriosis in shrimp (60). The LD_{50} of YDE17 was similar to that of *V. parahaemolyticus-pir*-201806 (61). To deal with *V. parahaemolyticus* infection, chemicals, antibiotics (62), phages (63), and probiotics (64) have been used. However, antibiotics have harmful effects on the health of consumers because they accumulate in breeding ponds after prolonged use, leading to the development of antibiotic-resistant bacteria (65). Although phages are natural agents, they are not often used, partially because their lytic activity is sensitive to temperature and salinity of culture water (66). As a probiotic, ZY1 offers advantages over antibiotics and phages with high safety, stability to heat, proteinase K, and pH. Compared with the most studied and commonly used probiotic candidates in shrimp aquaculture, such as LAB (67) and *Bacillus* spp. (68), which exhibit an RPS ranging from 51% to 76% (69–71), ZY1 has a relatively high RPS of 83.3%. Its *in vivo* protective effect could also be attributed to the iron deprivation effect, deduced from the higher survival rate of the ZY1/YDE17 group, compared to that of the YDE17/ZY1/$FeCl_3$ group. The unexpected lower survival rate of the YDE17/DP group might be due to the limitation in bioavailable iron for both pathogen and hosts (72), given that the shrimps with DP only showed a survival rate of 38%. Thus, *Glutamicibacter* sp. ZY1 may be a preferential candidate for the prevention of *Vibrio* infection.

In conclusion, ZY1, a bacterial isolate from a shrimp farm, exhibited significant inhibitory effects against a diverse of *Vibrio* spp. The inhibitory substances showed stability after thermal, proteinase K, and pH (6–10) treatments. Furthermore, the inhibitory effect of ZY1 and the effect of iron on the inhibitory assay indicated that ZY1 inhibited YDE17 through siderophore production. ZY1 produced the hydroxamate and α-hydroxycarboxylate siderophores, while YDE17 produced vibrioferrin siderophore. All our present results revealed that ZY1 won YDE17 for its higher ability to acquire iron through siderophores, thus exerting inhibitory effects on the growth of YDE17. Finally, artificial infection using shrimp as the experimental animals indicated that ZY1 had the potential to protect shrimp from *V. parahaemolyticus* infection.

ACKNOWLEDGMENTS

This work was financially supported by the Major Project of Science, Technology and Innovation 2025 in Ningbo City (2021Z007), the National Natural Science Foundation of China (42376103), the Natural Science Foundation of Ningbo City (2021J062), the Zhejiang Provincial Natural Science Foundation for Distinguished Young Scholar (LR20C190001), and the K.C. Wong Magna Fund in Ningbo University.

Zhili Shi: Conceptualization, Methodology, Data Curation, Software, Formal analysis, Validation, Visualization, Investigation, Resources, Writing–original draft, Writing–review and editing. Ya Li: Methodology, Investigation, Resources. Weibo Shi: Methodology,

Investigation. Zhixin Mu: Methodology, Investigation. Qingxi Han: Writing–review and editing, Funding acquisition. Weiwei Zhang: Conceptualization, Methodology, Data Curation, Visualization, Supervision, Project administration, Writing–review and editing, Funding acquisition.

AUTHOR AFFILIATIONS

[1]School of Marine Sciences, Ningbo University, Ningbo, China
[2]Key Laboratory of Aquacultural Biotechnology Ministry of Education, Ningbo University, Ningbo, China

AUTHOR ORCIDs

Zhili Shi http://orcid.org/0009-0004-1826-8272
Weiwei Zhang http://orcid.org/0000-0002-5678-2051

FUNDING

Funder	Grant(s)	Author(s)
Science and Technology Innovation 2025 Major Project of Ningbo	2021Z007	Qingxi Han
National Natural Science Foundation of China	42376103	Weiwei Zhang
Natural Science Foundation of Ningbo Municipality	2021J062	Weiwei Zhang
Science Fund for Distinguished Young Scholars of Zhejiang Province	LR20C190001	Weiwei Zhang
K. C. Wong Magna Fund in Ningbo University	NA	Weiwei Zhang

AUTHOR CONTRIBUTIONS

Zhili Shi, Conceptualization, Data curation, Formal analysis, Investigation, Methodology, Resources, Software, Validation, Visualization, Writing – original draft, Writing – review and editing | Ya Li, Investigation, Methodology, Resources | Weibo Shi, Investigation, Methodology | Zhixin Mu, Investigation, Methodology | Qingxi Han, Funding acquisition, Writing – review and editing | Weiwei Zhang, Conceptualization, Data curation, Funding acquisition, Methodology, Project administration, Supervision, Visualization, Writing – review and editing

DATA AVAILABILITY

The *Glutamicibacter* sp. ZY1 isolate was deposited into the China General Microbiological Culture Collection (CGMCC, Beijing, China) with accession number CGMCC no. 30798. Additional data will be made available on request.

ADDITIONAL FILES

The following material is available online.

Supplemental Material

Supplemental figures (AEM00009-25-s0001.docx). Figures S1 to S3.
Table S1 (AEM00009-25-s0002.docx). Bacterial purification and identification.

REFERENCES

1. Haris DI, Yaminudin J, Othman SH, Lim KC, Ismail I, Wulan Sari PD, Karim M. 2024. The use of commercial feed and microdiets incorporated with probiotics in Penaeid shrimp culture: a short review. Lat Am J Aquat Res 52:350–367. https://doi.org/10.3856/vol52-issue3-fulltext-3146
2. Gomez-Gil B, Roque A, Turnbull JF. 2000. The use and selection of probiotic bacteria for use in the culture of larval aquatic organisms. Aquaculture 191:259–270. https://doi.org/10.1016/S0044-8486(00)00431-2
3. Zhang XH, He X, Austin B. 2020. *Vibrio harveyi*: a serious pathogen of fish and invertebrates in mariculture. Mar Life Sci Technol 2:231–245. https://doi.org/10.1007/s42995-020-00037-z

4. Weber B, Chen C, Milton DL. 2010. Colonization of fish skin is vital for *Vibrio anguillarum* to cause disease. Environ Microbiol Rep 2:133–139. https://doi.org/10.1111/j.1758-2229.2009.00120.x
5. Deng Y, Chen C, Zhao Z, Huang X, Yang Y, Ding X. 2016. Complete genome sequence of *Vibrio alginolyticus* ZJ-T. Genome Announc 4:00912–00916. https://doi.org/10.1128/genomeA.00912-16
6. Broberg CA, Calder TJ, Orth K. 2011. *Vibrio parahaemolyticus* cell biology and pathogenicity determinants. Microbes Infect 13:992–1001. https://doi.org/10.1016/j.micinf.2011.06.013
7. Le H, LiHua D, JianJun F, Peng L, SongLin G. 2018. Immunogenicity study of an expressed outer membrane protein U of *Vibrio vulnificus* in Japanese eel (*Anguilla japonica*). J Appl Microbiol 125:1642–1654. https://doi.org/10.1111/jam.14068
8. Rico A, Oliveira R, McDonough S, Matser A, Khatikarn J, Satapornvanit K, Nogueira AJA, Soares A, Domingues I, Van den Brink PJ. 2014. Use, fate and ecological risks of antibiotics applied in tilapia cage farming in Thailand. Environ Pollut 191:8–16. https://doi.org/10.1016/j.envpol.2014.04.002
9. Santos L, Ramos F. 2018. Antimicrobial resistance in aquaculture: current knowledge and alternatives to tackle the problem. Int J Antimicrob Agents 52:135–143. https://doi.org/10.1016/j.ijantimicag.2018.03.010
10. Reverter M, Sarter S, Caruso D, Avarre J-C, Combe M, Pepey E, Pouyaud L, Vega-Heredía S, de Verdal H, Gozlan RE. 2020. Aquaculture at the crossroads of global warming and antimicrobial resistance. Nat Commun 11:1870. https://doi.org/10.1038/s41467-020-15735-6
11. Kalliomäki M, Antoine JM, Herz U, Rijkers GT, Wells JM, Mercenier A. 2010. Guidance for substantiating the evidence for beneficial effects of probiotics: prevention and management of allergic diseases by probiotics. J Nutr 140:713S–21S. https://doi.org/10.3945/jn.109.113761
12. Chauhan A, Singh R. 2019. Probiotics in aquaculture: a promising emerging alternative approach. Symbiosis 77:99–113. https://doi.org/10.1007/s13199-018-0580-1
13. Yaylacı EU. 2022. Isolation and characterization of *Bacillus* spp. from aquaculture cage water and its inhibitory effect against selected *Vibrio* spp. Arch Microbiol 204. https://doi.org/10.1007/s00203-021-02657-0
14. Sanches-Fernandes GMM, Sá-Correia I, Costa R. 2022. Vibriosis outbreaks in aquaculture: addressing environmental and public health concerns and preventive therapies using gilthead seabream farming as a model system. Front Microbiol 13:904815. https://doi.org/10.3389/fmicb.2022.904815
15. Farzanfar A. 2006. The use of probiotics in shrimp aquaculture. FEMS Immunol Med Microbiol 48:149–158. https://doi.org/10.1111/j.1574-695X.2006.00116.x
16. Kanmani P, Satish Kumar R, Yuvaraj N, Paari KA, Pattukumar V, Arul V. 2010. First identification of a novel probiotic bacterium *Streptococcus phocae* and its beneficial role in diseases control. J Int Med Res 3:45–51.
17. C De B, Meena DK, Behera BK, Das P, Das Mohapatra PK, Sharma AP. 2014. Probiotics in fish and shellfish culture: immunomodulatory and ecophysiological responses. Fish Physiol Biochem 40:921–971. https://doi.org/10.1007/s10695-013-9897-0
18. Noor Z, Noor M, Khan I, Khan SA. 2020. Evaluating the lucrative role of probiotics in the aquaculture using microscopic and biochemical techniques. Microsc Res Tech 83:310–317. https://doi.org/10.1002/jemt.23416
19. El-Saadony MT, Alagawany M, Patra AK, Kar I, Tiwari R, Dawood MAO, Dhama K, Abdel-Latif HMR. 2021. The functionality of probiotics in aquaculture: an overview. Fish Shellfish Immunol 117:36–52. https://doi.org/10.1016/j.fsi.2021.07.007
20. Ribeiro M, Simões M. 2019. Advances in the antimicrobial and therapeutic potential of siderophores. Environ Chem Lett 17:1485–1494. https://doi.org/10.1007/s10311-019-00887-9
21. Miller MJ, Zhu H, Xu Y, Wu C, Walz AJ, Vergne A, Roosenberg JM, Moraski G, Minnick AA, McKee-Dolence J, Hu J, Fennell K, Kurt Dolence E, Dong L, Franzblau S, Malouin F, Möllmann U. 2009. Utilization of microbial iron assimilation processes for the development of new antibiotics and inspiration for the design of new anticancer agents. Biometals 22:61–75. https://doi.org/10.1007/s10534-008-9185-0
22. Javvadi S, Pandey SS, Mishra A, Pradhan BB, Chatterjee S. 2018. Bacterial cyclic β-(1,2)-glucans sequester iron to protect against iron-induced toxicity. EMBO Rep 19:172–186. https://doi.org/10.15252/embr.201744650
23. Yang M, Zhang J, Liang Q, Pan G, Zhao J, Cui M, Zhao XQ, Zhang QZ, Xu D. 2019. Antagonistic activity of marine *Streptomyces* sp. S073 on pathogenic *Vibrio parahaemolyticus*. Fish Sci 85:533–543. https://doi.org/10.1007/s12562-019-01309-z
24. Wang WL, Chi ZM, Chi Z, Li J, Wang XH. 2009. Siderophore production by the marine-derived *Aureobasidium pullulans* and its antimicrobial activity. Bioresour Technol 100:2639–2641. https://doi.org/10.1016/j.biortech.2008.12.010
25. Zhang W, Liang W, Li C. 2016. Inhibition of marine *Vibrio* sp. by pyoverdine from *Pseudomonas aeruginosa* PA1. J Hazard Mater 302:217–224. https://doi.org/10.1016/j.jhazmat.2015.10.003
26. Chakraborty K, Francis A, Chakraborty RD, Asharaf S, Kizhakkekalam VK, Paulose SK. 2021. Marine macroalga-associated heterotrophic *Bacillus velezensis*: a novel antimicrobial agent with siderophore mode of action against drug-resistant nosocomial pathogens. Arch Microbiol 203:5561–5575. https://doi.org/10.1007/s00203-021-02513-1
27. Aranda CP, Valenzuela C, Barrientos J, Paredes J, Leal P, Maldonado M, Godoy FA, Osorio CG. 2012. Bacteriostatic anti-*Vibrio parahaemolyticus* activity of *Pseudoalteromonas* sp. strains DIT09, DIT44 and DIT46 isolated from Southern Chilean intertidal *Perumytilus purpuratus*. World J Microbiol Biotechnol 28:2365–2374. https://doi.org/10.1007/s11274-012-1044-z
28. Zhang D, Feng Y, Chu M, Dai Y, Jiang L, Li H. 2024. Anti-vibriosis bioactive molecules from marine-derived variant *Streptomyces* sp. ZZ741A. Nat Prod Res:1–12. https://doi.org/10.1080/14786419.2024.2321487
29. Lane DJ. 1991. 16S/23S rRNA sequencing. In Nucleic acid techniques in bacterial systematics
30. Saitou N, Nei M. 1987. The neighbor-joining method: a new method for reconstructing phylogenetic trees. Mol Biol Evol 4:406–425. https://doi.org/10.1093/oxfordjournals.molbev.a040454
31. Ren W, Xue B, Cao F, Long H, Zeng YH, Zhang X, Cai XN, Huang AY, Xie ZY. 2022. Multi-costimulatory pathways drive the antagonistic *Pseudoalteromonas piscicida* against the dominant pathogenic *Vibrio harveyi* in mariculture: insights from proteomics and metabolomics. Microbiol Spectr 10:e0244422. https://doi.org/10.1128/spectrum.02444-22
32. Tang BL, Yang J, Chen XL, Wang P, Zhao HL, Su HN, Li CY, Yu Y, Zhong S, Wang L, Lidbury I, Ding HT, Wang M, McMinn A, Zhang XY, Chen Y, Zhang YZ. 2020. A predator-prey interaction between a marine *Pseudoalteromonas* sp. and gram-positive bacteria. Nat Commun 11:285. https://doi.org/10.1038/s41467-019-14133-x
33. Ma M, Zhuang Y, Chang L, Xiao L, Lin Q, Qiu Q, Chen D, Egan S, Wang G. 2023. Naturally occurring beneficial bacteria *Vibrio alginolyticus* X-2 protects seaweed from bleaching disease. MBio 14:e0006523. https://doi.org/10.1128/mbio.00065-23
34. Mandal H, Bagchi T. 2018. *In vitro* screening of indigenous *Lactobacillus* isolates for selecting organisms with better health-promoting attributes. Appl Biochem Biotechnol 185:1060–1074. https://doi.org/10.1007/s12010-018-2709-3
35. Rajasekaran G, Dinesh Kumar S, Nam J, Jeon D, Kim Y, Lee CW, Park I-S, Shin SY. 2019. Antimicrobial and anti-inflammatory activities of chemokine CXCL14-derived antimicrobial peptide and its analogs. Biochim Biophys Acta Biomembr 1861:256–267. https://doi.org/10.1016/j.bbamem.2018.06.016
36. Payne SM. 1994. Detection, isolation, and characterization of siderophores. Methods Enzymol 235:329–344. https://doi.org/10.1016/0076-6879(94)35151-1
37. Schwyn B, Neilands JB. 1987. Universal chemical assay for the detection and determination of siderophores. Anal Biochem 160:47–56. https://doi.org/10.1016/0003-2697(87)90612-9
38. Arnow LE. 1937. Colorimetric determination of the components of 3,4-dihydrophenylalanine tyrosine mixtures. Journal of Biological Chemistry 118:531–537. https://doi.org/10.1016/S0021-9258(18)74509-2
39. Neilands JB. 1981. Microbial iron compounds. Annu Rev Biochem 50:715–731. https://doi.org/10.1146/annurev.bi.50.070181.003435
40. Pérez-Miranda S, Cabirol N, George-Téllez R, Zamudio-Rivera LS, Fernández FJ. 2007. O-CAS, a fast and universal method for siderophore detection. J Microbiol Methods 70:127–131. https://doi.org/10.1016/j.mimet.2007.03.023
41. Tanabe T, Funahashi T, Nakao H, Miyoshi S-I, Shinoda S, Yamamoto S. 2003. Identification and characterization of genes required for biosynthesis and transport of the siderophore vibrioferrin in *Vibrio parahaemolyticus*. J Bacteriol 185:6938–6949. https://doi.org/10.1128/JB.185.23.6938-6949.2003

42. Hamilton MA, Russo RC, Thurston RV. 1978. Trimmed Spearman-Karber method for estimating median lethal concentrations in bioassays. Environ Sci Technol 12:417–417. https://doi.org/10.1021/es60140a017
43. Liu H, Wang S, Cai Y, Guo X, Cao Z, Zhang Y, Liu S, Yuan W, Zhu W, Zheng Y, Xie Z, Guo W, Zhou Y. 2017. Dietary administration of *Bacillus subtilis* HAINUP40 enhances growth, digestive enzyme activities, innate immune responses and disease resistance of tilapia, *Oreochromis niloticus*. Fish Shellfish Immunol 60:326–333. https://doi.org/10.1016/j.fsi.2016.12.003
44. Bernal MG, Campa-Córdova ÁI, Saucedo PE, González MC, Marrero RM, Mazón-Suástegui JM. 2015. Isolation and *in vitro* selection of actinomycetes strains as potential probiotics for aquaculture. Vet World 8:170–176. https://doi.org/10.14202/vetworld.2015.170-176
45. Das S, Ward LR, Burke C. 2008. Prospects of using marine actinobacteria as probiotics in aquaculture. Appl Microbiol Biotechnol 81:419–429. https://doi.org/10.1007/s00253-008-1731-8
46. Mondal H, Thomas J. 2022. Isolation and characterization of a novel *Actinomycete* isolated from marine sediments and its antibacterial activity against fish pathogens. Antibiotics (Basel) 11:1546. https://doi.org/10.3390/antibiotics11111546
47. Busse HJ. 2016. Review of the taxonomy of the genus *Arthrobacter*, emendation of the genus *Arthrobacter sensu lato*, proposal to reclassify selected species of the genus *Arthrobacter* in the novel genera *Glutamicibacter* gen. nov., *Paeniglutamicibacter* gen. nov., *Pseudoglutamicibacter* gen. nov., *Paenarthrobacter* gen. nov. and *Pseudarthrobacter* gen. nov., and emended description of *Arthrobacter roseus*. Int J Syst Evol Microbiol 66:9–37. https://doi.org/10.1099/ijsem.0.000702
48. Karthik Y, Ishwara Kalyani M, Krishnappa S, Devappa R, Anjali Goud C, Ramakrishna K, Wani MA, Alkafafy M, Hussen Abduljabbar M, Alswat AS, Sayed SM, Mushtaq M. 2023. Antiproliferative activity of antimicrobial peptides and bioactive compounds from the mangrove *Glutamicibacter mysorens*. Front Microbiol 14:1096826. https://doi.org/10.3389/fmicb.2023.1096826
49. Asif T, Javed U, Zafar SB, Ansari A, Ul Qader SA, Aman A. 2020. Bioconversion of colloidal chitin using novel chitinase from *Glutamicibacter uratoxydans* exhibiting anti-fungal potential by hydrolyzing chitin within fungal cell wall. Waste Biomass Valor 11:4129–4143. https://doi.org/10.1007/s12649-019-00746-2
50. Knobloch S, Skírnisdóttir S, Dubois M, Kolypczuk L, Leroi F, Leeper A, Passerini D, Marteinsson VÞ. 2022. Impact of putative probiotics on growth, behavior, and the gut microbiome of farmed Arctic Char (*Salvelinus alpinus*). Front Microbiol 13:912473. https://doi.org/10.3389/fmicb.2022.912473
51. Li X, Yi Y, Wu J, Yang Q, Tan B, Chi S. 2022. Effects of plant-derived Glycerol Monolaurate (GML) additive on the antioxidant capacity, anti-inflammatory ability, muscle nutritional value, and intestinal flora of hybrid grouper (*Epinephelus fuscoguttatus* ♀ × *Epinephelus lanceolatus* ♂). Metabolites 12:1089. https://doi.org/10.3390/metabo12111089
52. Xu W, Lv Z, Guo Q, Deng Z, Yang C, Cao Z, Li Y, Huang CF, Wu ZZ, Chen SJ, He YH, Sun JJ, Liu YY, Gan L. 2023. Selective antagonism of *Lactiplantibacillus plantarum* and *Pediococcus acidilactici* against *Vibrio* and *Aeromonas* in the bacterial community of *Artemia nauplii*. Microbiol Spectr 11:e0053323. https://doi.org/10.1128/spectrum.00533-23
53. Terra L, Ratcliffe N, Castro HC, Vicente ACP, Dyson P. 2021. Biotechnological potential of *Streptomyces* siderophores as new antibiotics. Curr Med Chem 28:1407–1421. https://doi.org/10.2174/0929867327666200510235512
54. Fu B, Olawole O, Beattie GA. 2021. Biological control and microbial ecology draft genome sequence data of *Glutamicibacter* sp. FBE-19, a bacterium antagonistic to the plant pathogen *Erwinia tracheiphila*. Phytopathology 111:765–768. https://doi.org/10.1094/PHYTO-09-20-0380-A
55. Chen YA, Chiu WC, Wang TY, Wong HC, Tang CT. 2024. Isolation and characterization of an antimicrobial *Bacillus subtilis* strain O-741 against *Vibrio parahaemolyticus*. PLoS ONE 19:e0299015. https://doi.org/10.1371/journal.pone.0299015
56. Lv R, Li B, Xiao Y, Zhang J, Mai Y, Hu X, Chen J. 2023. Isolation and characterization of a lipopeptide-producing *Bacillus* sp. strain JK08 with antagonistic activity against *Vibrio parahaemolyticus*. J Appl Microbiol 134:lxad084. https://doi.org/10.1093/jambio/lxad084
57. Khouadja S, Haddaji N, Hanchi M, Bakhrouf A. 2017. Selection of lactic acid bacteria as candidate probiotics for *Vibrio parahaemolyticus* depuration in pacific oysters (*Crassostrea gigas*). Aquac Res 48:1885–1894. https://doi.org/10.1111/are.13026
58. Thode SK, Kahlke T, Robertsen EM, Hansen H, Haugen P. 2015. The immediate global responses of *Aliivibrio salmonicida* to iron limitations. BMC Microbiol 15:9. https://doi.org/10.1186/s12866-015-0342-7
59. Saha R, Saha N, Donofrio RS, Bestervelt LL. 2013. Microbial siderophores: a mini review. J Basic Microbiol 53:303–317. https://doi.org/10.1002/jobm.201100552
60. de Souza Valente C, Wan AHL. 2021. *Vibrio* and major commercially important vibriosis diseases in decapod crustaceans. J Invertebr Pathol 181:107527. https://doi.org/10.1016/j.jip.2020.107527
61. Yang F, Xu L, Huang W, Li F. 2022. Highly lethal *Vibrio parahaemolyticus* strains cause acute mortality in *Penaeus vannamei* post-larvae. Aquaculture 548:737605. https://doi.org/10.1016/j.aquaculture.2021.737605
62. Noman E, Al-Gheethi A, Radin Mohamed RMS, Talip B, Al-Sahari M, Al-Shaibani M. 2021. Quantitative microbiological risk assessment of complex microbial community in prawn farm wastewater and applicability of nanoparticles and probiotics for eliminating of antibiotic-resistant bacteria. J Hazard Mater 419:126418. https://doi.org/10.1016/j.jhazmat.2021.126418
63. Żaczek M, Weber-Dąbrowska B, Górski A. 2020. Phages as a cohesive prophylactic and therapeutic approach in aquaculture systems. Antibiotics (Basel) 9:564. https://doi.org/10.3390/antibiotics9090564
64. Yilmaz S, Yilmaz E, Dawood MAO, Ringø E, Ahmadifar E, Abdel-Latif HMR. 2022. Probiotics, prebiotics, and synbiotics used to control vibriosis in fish: a review. Aquaculture 547:737514. https://doi.org/10.1016/j.aquaculture.2021.737514
65. Zhang YB, Li Y, Sun XL. 2011. Antibiotic resistance of bacteria isolated from shrimp hatcheries and cultural ponds on Donghai island, China. Mar Pollut Bull 62:2299–2307. https://doi.org/10.1016/j.marpolbul.2011.08.048
66. Alagappan K, Karuppiah V, Deivasigamani B. 2016. Protective effect of phages on experimental *V. parahaemolyticus* infection and immune response in shrimp (Fabricius, 1798). Aquaculture 453:86–92. https://doi.org/10.1016/j.aquaculture.2015.11.037
67. Balcázar JL, Vendrell D, de Blas I, Ruiz-Zarzuela I, Muzquiz JL, Girones O. 2008. Characterization of probiotic properties of lactic acid bacteria isolated from intestinal microbiota of fish. Aquaculture 278:188–191. https://doi.org/10.1016/j.aquaculture.2008.03.014
68. Amoah K, Huang QC, Tan BP, Zhang S, Chi SY, Yang QH, Liu HY, Dong XH. 2019. Dietary supplementation of probiotic *Bacillus coagulans* ATCC 7050, improves the growth performance, intestinal morphology, microflora, immune response, and disease confrontation of Pacific white shrimp, *Litopenaeus vannamei*. Fish Shellfish Immunol 87:796–808. https://doi.org/10.1016/j.fsi.2019.02.029
69. Amoah K, Dong XH, Tan BP, Zhang S, Chi SY, Yang QH, Liu HY, Yang YZ, Zhang HT. 2020. Administration of probiotic *Bacillus licheniformis* induces growth, immune and antioxidant enzyme activities, gut microbiota assembly and resistance to *Vibrio parahaemolyticus* in *Litopenaeus vannamei*. Aquacult Nutr 26:1604–1622. https://doi.org/10.1111/anu.13106
70. Chomwong S, Charoensapsri W, Amparyup P, Tassanakajon A. 2018. Two host gut-derived lactic acid bacteria activate the proPO system and increase resistance to an AHPND-causing strain of *Vibrio parahaemolyticus* in the shrimp *Litopenaeus vannamei*. Dev Comp Immunol 89:54–65. https://doi.org/10.1016/j.dci.2018.08.002
71. Du Y, Xu W, Wu T, Li H, Hu X, Chen J. 2022. Enhancement of growth, survival, immunity and disease resistance in *Litopenaeus vannamei*, by the probiotic, *Lactobacillus plantarum* Ep-M17. Fish Shellfish Immunol 129:36–51. https://doi.org/10.1016/j.fsi.2022.08.066
72. Doherty CP. 2007. Host-pathogen interactions: the role of iron. J Nutr 137:1341–1344. https://doi.org/10.1093/jn/137.5.1341